# Translational Diffusion of Cyclic Peptides Measured Using Pulsed-Field Gradient NMR

*Conan K. Wang*[1*], *Susan E. Northfield*[1], *Joakim E. Swedberg*[1], *Peta J. Harvey*[1], *Alan M. Mathiowetz*[2], *David A. Price*[2], *Spiros Liras*[2], *David J. Craik*[1]

[1]Institute for Molecular Bioscience, the University of Queensland, Brisbane, Queensland, 4072, Australia

[2]Worldwide Medicinal Chemistry, CVMED, Pfizer, 610 Main Street, Cambridge, MA 02139, USA

*Corresponding Author:

Dr Conan K Wang

Institute for Molecular Bioscience,

The University of Queensland,

Brisbane, Qld, 4072, Australia

Tel: 61-7-3346 2014

Fax: 61-7-3346 2101

e-mail: c.wang@imb.uq.edu.au

**Running Title:** Diffusion of cyclic peptides

**Abstract**

Cyclic peptides are increasingly being recognized as valuable templates for drug discovery or design. To facilitate efforts in the structural characterization of cyclic peptides, we explore the use of pulse-field gradient experiments as a convenient and non-invasive approach for characterizing their diffusion properties in solution. We present diffusion coefficient measurements of five cyclic peptides, including dichC, SFTI-1, cVc1.1, kB1 and kB2. These peptides range in size from six to 29 amino acids and have various therapeutically interesting activities. We explore the use of internal standards, such as dioxane and acetonitrile, to evaluate the hydrodynamic radius from the diffusion coefficient, and show that 2,2-dimethyl-2-silapentane-5-sulfonic acid, a commonly used chemical shift reference, can be used as an internal standard to avoid spectral overlap issues and simplify data analysis. The experimentally measured hydrodynamic radii correlate with increasing molecular weight and *in silico* predictions. We further applied diffusion measurements to characterize the self-association of kB2 and showed that it forms oligomers in a concentration-dependent manner, which may be relevant to its mechanism of action. Diffusion coefficient measurements appear to have broad utility in cyclic peptide structural biology, allowing for the rapid characterization of their molecular shape in solution.

**Keywords:** cyclic peptide, NMR, hydrodynamic radius, self-association

## Introduction

Pulsed-field gradient NMR (PFG-NMR) is a convenient and non-invasive technique for characterizing translational motion of biomolecular systems.[1] Some prominent applications of PFG-NMR include monitoring of protein association,[2-6] evaluation of protein diffusion under the crowded conditions found in cells,[7] characterization of protein-ligand interactions,[8,9] and determination of the size and shape of protein-micelle complexes.[10,11] Compared to other methods used to derive similar biophysical parameters, such as ultracentrifugation, quasi-elastic light scattering, small-angle X-ray scattering, or small-angle neutron scattering, PFG-NMR has the advantage that the measurements can be carried out under conditions that closely mimic those used for NMR structure determination and other biophysical/structural studies in solution.

PFG-NMR can be used to measure the translational diffusion constant, $D_T$, of molecules of various sizes. For spherical particles undergoing Brownian motion, their hydrodynamic radius, $R_h$, can be derived directly from $D_T$ according to Stokes-Einstein relationship.[12] $R_h$ is an important parameter that describes the effects of hydration and shape on the apparent size of a molecule and is different by definition to other radii terms used to describe molecular size (Figure 1). Once the $D_T$ is obtained from a PFG-NMR experiment, $R_h$ can be determined by (i) correcting the measured diffusion coefficients for temperature and solvent viscosity and extrapolating to zero solute concentration, or (ii) introducing a small organic molecule as an internal standard against which measured diffusion coefficients are compared. Of the two approaches, the use of internal standards is arguably more robust and straightforward because it can be readily applied to a range of sample mixtures.[13]

Herein, we explore the use of PFG-NMR to study the translational diffusion of cyclic peptides, a class of molecules attracting increasing attention as pharmaceutical or agricultural agents.[14-16] A selection of these peptides with therapeutic and agrochemical potential were examined in this study (Table 1), comprising four naturally-occurring macrocyclic peptides and one synthetically cyclized peptide. Aside from their interesting natural bioactivities, cyclic peptides are increasingly being recognized as an important and under-exploited

structural class for drug design and development.[17] Because of their size and constrained conformations, they have advantages over linear peptides, including increased stability and binding affinities, potentially leading to improved pharmacokinetic properties. For example, a cyclized analogue of a venom peptide from *Conus victoriae*, cVc1.1, displayed potent oral activity against neuropathic pain whereas the linear analogue was not active when delivered orally.[18] Other cyclic peptides, such as SFTI-1[19] and cyclotides,[20,21] are promising molecular templates for stabilizing biologically active linear peptide sequences. For example, kalata B1 has been modified using molecular grafting to engineer stable immuno-modulatory peptides for the treatment of multiple sclerosis[22] and orally active peptide bradykinin B1 receptor antagonists for inflammatory pain.[23]

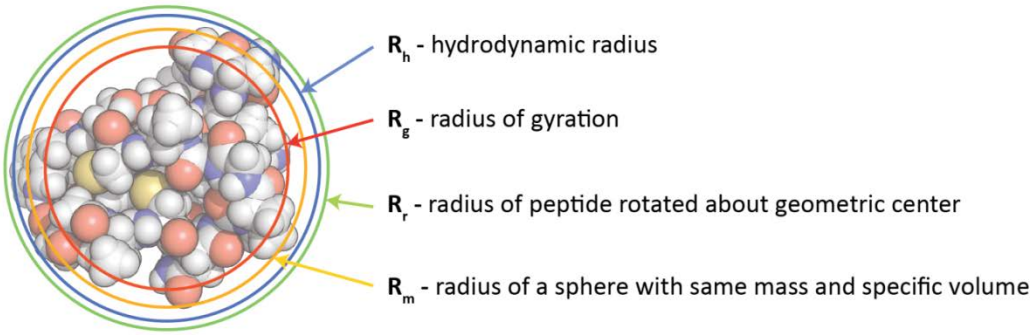


**Figure 1:** Comparison of the various radius terms used to characterize peptides. The peptide is shown as a sphere representation. The various radii parameters are shown illustratively as circles of different colors.

In this study, PFG-NMR was used to provide rapid structural information on cyclic peptides. Although PFG-NMR has been used to study the translation diffusion of short linear peptides[24] and some aspects of cyclic peptide structure,[25-27] we provide here a detailed investigation of the PFG-NMR method and its application to a range of cyclic peptides with different amino acid and disulfide-bond content, recognizing the growing need for useful tools in cyclic peptide structural biology. We investigate the use of internal standards to interpret acquired diffusion coefficients. We measure the $R_h$ of a range of cyclic peptides with varying molecular weights and further apply this approach to the characterization of self-association (which may be relevant to the peptide's mode of action/biological activity). We compare our observed data to computational

predictions relating to the size and shape of the cyclic peptides to validate our method. This study provides a foundation for future studies on the behavior of cyclic peptides in solution.

**Table 1:** Sequence, classification and activities of cyclic peptides studied in this work.

| Peptide[a] | Sequence[b] | Peptide Class[c] | Activity/Applications |
|---|---|---|---|
| **dichC** *(0 SS)* | *cyclo(*GTFLYA*)* | Orbitides (*Stellaria dichotoma*) | Inhibitory activity against lymphocytic leukemia cells[28] |
| **SFTI-1** *(1 SS)* | *cyclo(*GR**C**TKSIPPI**C**FPD*)* | BBI-like trypsin inhibitor (*Helianthus annus*) | Trypsin inhibition,[29] drug design scaffold[19] |
| **cVc1.1** *(2 SS)* | *cyclo(*G**CC**SDPR**C**NYDHPEI**C**GGAAGG*)* | Conotoxin (*synthetically cyclized*) | Oral activity against neuropathic pain[18] |
| **kB1** *(3 SS)* | *cyclo(*GLPV**C**GET**C**VGGT**C**NTPG**C**T**C**SWPV**C**TRN*)* | Cyclotide (*Oldenlandia affinis*) | Uterotonic,[30] pesticidal,[31-33] anti-HIV,[34] immunosuppressant,[35] drug design scaffold[21] |
| **kB2** *(3 SS)* | *cyclo(*GLPV**C**GET**C**FGGT**C**NTPG**C**S**C**TWPI**C**TRD*)* | Cyclotide (*Oldenlandia affinis*) | Nematocidal,[31] pesticidal,[32,33] drug design scaffold[21] |

[a] The peptides used in this study include dichotomin C (dich C), sunflower trypsin inhibitor-1 (SFTI-1), cyclic Vc1.1 (cVc1.1), kalata B1 (kB1), kalata B2 (kB2). The number of disulfide bonds is indicated in parentheses.

[b] The peptides have a head-to-tail cyclic backbone. The cysteine residues are shown in bold and the disulfide bond connectivity indicated

[c] The peptide family and the original source of the peptide

**Experimental Methods**

*General*

N-terminal protected amino acids, resin and coupling agents were purchased from ChemImpex International, and all other reagents were purchased from Auspep, Merck and Sigma, and used without further purification. $D_2O$ (D, 99.96%) and acetonitrile-d3 (D, 99.8%) were purchased from Cambridge Isotope Laboratories, Inc.

*Peptide synthesis*

DichC was synthesized on 2-chlorotrityl chloride (2CTC) resin on 0.25 mmol scale using Fluorenylmethyloxycarbonyl chloride (Fmoc)-chemistry. Couplings were performed using 4 equiv. Fmoc-protected amino acid, 3 equiv. HCTU (O-(6-Chlorobenzotriazol-1-y1)-N,N,N',N'-tetramethyluronium hexafluorophosphate) and 6 equiv. N,N-diisopropylethylamine (DIPEA) in dimethylformamide (DMF) (0.1 M in amino acid) for 2 x 10 min. Fmoc deprotection was carried out with 30% (v/v) piperidine in DMF. After each coupling and deprotection step, the resin was washed with DMF (3×), dichloromethane (DCM) (3×) and DMF (3×). DichC was cleaved from the resin using 1% (v/v) TFA (trifluoroacetic acid) in DCM (dichloromethane). Head-to-tail cyclization was performed in DMF with 3 equiv. HATU and 6 equiv. DIPEA. Following removal of the solvent, side-chain protecting groups were removed in 94:3:3 TFA/TIPS (triisopropylsilane)/water. After cyclization, the peptides were purified by reverse-phase (RP) preparative high performance liquid chromatography (HPLC). Purity of fractions was assessed using ESI-MS and analytical HPLC.

SFTI-1, cVc1.1, kB1 and kB2 were synthesized on 0.5 mmol scale using *tert*-butyloxycarbonyl (Boc)-chemistry. Peptides were assembled on Boc-Gly-PAM resin via thioester linker, allowing cyclization by native chemical ligation. Following peptide cleavage from the resin using hydrofluoric acid (HF), the crude peptides were purified by RP-HPLC. Cyclization and oxidation were subsequently carried out in a one-pot reaction in $NH_4HCO_3$ buffer (0.1 M, pH 8.5) overnight. Peptides were purified by preparative RP-HPLC and purity of fractions assessed by ESI-MS and analytical HPLC.

*NMR sample preparation*

NMR samples were prepared by dissolving dried peptide in 100% (v/v) $D_2O$ or 30% (v/v) acetonitrile-d3, 70% (v/v) $D_2O$ to a concentration of ~1 mM and a volume of 550 μl. Concentration of the peptides were determined based on their absorbance at 280 nm. Concentrated samples of 1,4-dioxane (1% v/v dioxane in $D_2O$) or 2,2-dimethyl-2-silapentane-5-sulfonic acid (DSS; 10 mg/ml in $D_2O$) were prepared and added to the samples as internal standards. Unless otherwise specified, 1.5 μl of dioxane and 7.5 μl of DSS standards were added to samples.

The pH of samples was measured using a micro pH combination electrode (Sigma-Aldrich) and adjusted using small amounts of concentrated DCl and NaOD. pH* is the direct reading of the pH in a $D_2O$ solution of the $H_2O$-calibrated pH-meter. The conversion of pH* into pD was accomplished by adding a constant of 0.4.[36]

*PFG-NMR spectroscopy*

PFG-NMR spectra were acquired at 25ºC (or other temperatures as indicated) on a Bruker Avance-500 MHz spectrometer. A PFG longitudinal eddy-current delay (LED) pulse sequence incorporating bipolar phases was used to reduce the effects of eddy currents,[37] which are induced in the metal structures of the magnet and probe by gradient pulses. This pulse sequence has been widely used for the study of translational diffusion of proteins. All diffusion measurements were recorded using pseudo-two-dimensional experiments, acquiring 32 spectra across a range of gradient strengths ranging from 2% to 95% of the maximum gradient strength. A sine bell gradient shape was used and the diffusion time was set to 100 ms and the gradient length ranged from 750 to 1250 ms. Spectra were recorded using 32, 64 or 128 scans. The diffusion measurements were performed in triplicates. The gradient coil of the probe head was calibrated using a 5 mm NMR tube using 99.96% $D_2O$, which gave a $D_T$ of HDO (99.96% $D_2O$) of 2.00 x $10^{-9}$ $m^2s^{-1}$ at 298 K.

*Translational diffusion induced signal attenuation and data processing*

Signal attenuation in the presence of a single pair of pulsed field gradients is given by

***Equation 1:***

$$I = I_0 e^{(-\gamma^2 g^2 D_T \delta^2 \left(\Delta - \frac{\delta}{3}\right))}$$

where γ is the gyromagnetic ratio and *g*, δ and Δ are the amplitude, duration and separation of the single pair of gradient pulses, respectively.[38] It is worth noting that different shapes of the gradient can affect the form of the equation above.[39,40] All spectra were processed using TOPSPIN (Bruker). An exponential window function with 2 Hz line broadening was applied before Fourier transformation, followed by baseline correction. Data analyses were accomplished using the relaxation T1/T2 routine. For each measurement, at least four peaks across the spectrum were used in the fitting and the average value was reported.

*Internal standard for diffusion measurements*

For spherical particles undergoing Brownian motion, the Stokes-Einstein relationship can be used to relate the hydrodynamic radius, $R_h$, to $D_T$.[12]

***Equation 2:***

$$D_T = \frac{k_B T}{6\pi\eta R_h}$$

where *T* is the temperature (in Kelvin), $k_B$ is Boltzmann's constant, and $\eta$ is the solvent viscosity.

Small molecule internal viscosity standards can be used to avoid complexities arising from variations in sample conditions. An internal viscosity standard with a known $R_h$ for the same solvent (and at the same temperature) as that used for the sample peptide can be used to evaluate the effective hydrodynamic radius of the peptide according to Equation 3.[13] Previous studies have used dioxane as an internal viscosity

standard; the hydrodynamic radius of dioxane in an aqueous buffer at 298 K has been determined to be 2.12 Å.[13]

***Equation 3:***

$$R_h = R_h^{standard} \times \frac{D_T^{standard}}{D_T}$$

When comparing diffusion coefficients measured from two different solvents (i.e. solvent A and solvent B), Equation 4 can be used to account for the differences in solvent viscosities. At 298 K, the viscosity of $H_2O$ has been reported to be 0.89 cP and $D_2O$ is 1.10 cP.[41] The viscosity of 30% (v/v) acetonitrile, 70% (v/v) $H_2O$ is 0.92 cP at 298 K.[42] We assume that the ratio of the viscosities of 100% (v/v) $H_2O$ to 30% (v/v) acetonitrile, 70% (v/v) $H_2O$ is equivalent to the ratio of viscosities of 100% (v/v) $D_2O$ to 30% (v/v) acetonitrile-d3, 70% (v/v) $D_2O$; therefore, we estimate the viscosity of 30% (v/v) acetonitrile-d3, 70% (v/v) $D_2O$ to be 1.14 cP.

***Equation 4:***

$$R_h^B = R_h^A \times \frac{D_T^A}{D_T^B} \times \frac{\eta^A}{\eta^B}$$

*Molecular dynamics simulation*

Molecular dynamics simulations of cyclic peptides were generated in water and 30% (v/v) acetonitrile. The structures of SFTI-1 (PDB ID: 1SFI), cVc1.1 (P04244; http://www.conoserver.org), kB1 (PDB ID: 1NB1) were used as starting structures. The structure of dichC was modelled using YASARA. Force field parameters for acetonitrile were obtained from SwissParam (http://www.swissparam.ch/). Each peptide was equilibrated using a stepwise relaxation procedure. All heavy-atoms were harmonically restrained with a force constant of 2 kcal $mol^{-1}$ $Å^{-2}$ before a conjugate gradient minimization of 5000 steps was applied using NAMD 2.7 and CHARMM27 force field parameters. The simulation was heated to 298 K before gradual release over 2.5 ns under NPT conditions and periodic boundary conditions. A Langevin thermostat with a damping coefficient of 0.5 $ps^{-1}$ was used to maintain the system temperature. The system pressure was

maintained at 1 atm using a Langevin piston barostat. The particle mesh Ewald algorithm was used to compute long-range electrostatic interactions at every time step and non-bonded interactions were truncated smoothly between 10.5 Å and 12 Å. All covalent hydrogen bonds were constrained by the SHAKE algorithm (or the SETTLE algorithm for water), permitting an integration time step of 2 fs. Production runs of 10 ns were carried out using ACEMD. These simulations were performed under NVT with otherwise identical force field and simulation parameters as above. Coordinates were saved every 500 simulation steps producing 10000 frames per run.

*Calculation of biophysical properties of cyclic peptides*

The sequences of the cyclic peptides were obtained from either CyBase, a database of cyclic proteins,[15] or from ConoServer, a database of venom peptides.[43] The molecular weights, MW, of the peptides were calculated using the Digest Peptide tool on CyBase.[15]

Diffusion coefficients of the peptides in water (i.e. solvent density of 1 g $cm^{-3}$ and viscosity of 0.89 cP) were predicted using the program HYDROPRO[44] with mode 2 (i.e. shell-model from residue-level) using the average conformation of the peptides from the molecule dynamics simulation.

**Results & Discussion**

Diffusion constants can provide valuable information about the conformation of biomolecules in solution. We investigated PFG-NMR as a convenient and non-invasive approach for evaluating the diffusion constants of cyclic peptides and subsequently deriving their hydrodynamic radii. The methods developed in this work will be relevant to the growing number of structure-guided projects on cyclic peptides, their mechanism of action and potential therapeutic applications.[45]

As mentioned in the Introduction, derivation of $R_h$ from the measured $D_T$ can be achieved using Equation 2 by adjusting the measured $D_T$ for temperature and solvent viscosity and extrapolating to zero solute concentration to correct for the effects of the solute on solvent viscosity. To illustrate this, we measured the $D_T$ of dioxane at various concentrations in $D_2O$ and evaluated the $D_T$ of dioxane at infinite dilution to be $9.63 \times 10^{-10}$ $m^2$ $s^{-1}$ by extrapolation of the measured values to zero dioxane concentration (Supplementary Figure S1). Using Equation 2, the $R_h$ of dioxane was calculated to be 2.06 Å, which is similar to the reported value of 2.12 Å.[13] Alternatively, it has been proposed that $R_h$ can be derived from the measured $D_T$ using Equation 3 and an internal standard with a known $R_h$ and $D_T$ (Experimental Methods). Dioxane and other small molecule internal standards have been used in previous studies on proteins and linear peptides.[6]

Figure 2 shows 1D $^1H$ NMR spectra of the cyclic peptides in this study with and without the addition of dioxane and DSS. One complication arises when the dioxane resonance overlaps with the peptide resonance at 3.7 ppm. The observed attenuation of the dioxane signal peak is then distorted by the diffusion properties of the peptide. One solution is to fit the signal attenuation to a two component decay function,[12] as shown in Supplementary Figure S2. An alternative is to use an internal standard which has a resonance that does not overlap with any peptide resonance peaks. For this purpose, we investigated the utility of DSS, which typically lies far up-field in NMR spectra and is commonly used as a chemical shift reference.

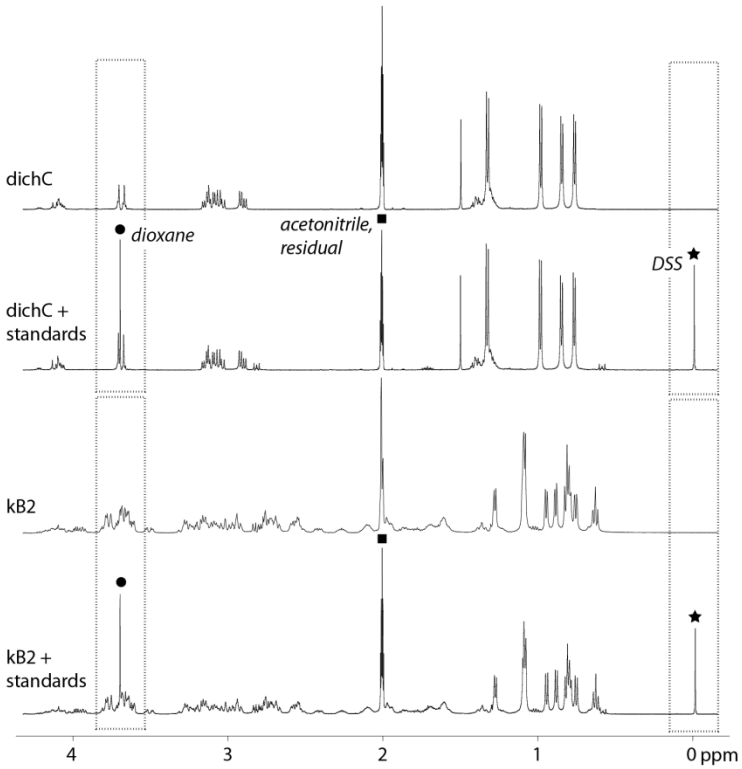


**Figure 2:** 1D $^{1}$H NMR spectra of cyclic peptides studies in this work (dichC and kB2) with and without the addition of small molecule internal standards (dioxane and DSS indicated by a circle and a star, respectively). The spectra were acquired for peptides in 30% (v/v) acetonitrile-d3 and 70% (v/v) $D_2O$ at 298 K with a pD ~4. The spectra were referenced to DSS at 0 ppm.

To characterize whether DSS is a suitable small molecule internal standard, its diffusion properties were measured in $D_2O$ and in the presence of dioxane at varying temperatures and solvent pD. As shown in Table 2, the $D_T$ of DSS remains relatively consistent at around $5.95 \times 10^{-10}$ m$^2$ s$^{-1}$over a range of pD values from 3.7 to 7.4. The $D_T$ of dioxane is around $9.61 \times 10^{-10}$ m$^2$ s$^{-1}$ over the same pD range, giving a consistent ratio of the two $D_T$ values of about 1.62. According to Equation 3, the $R_h$ of DSS in $D_2O$ at 298 K was evaluated to be 3.34 Å. The diffusion properties of DSS were also measured in 30% (v/v) acetonitrile-d3, 70% (v/v) $D_2O$ at varying temperatures and solvent pD (Table 3). Similar to the result obtained in 100% (v/v) $D_2O$, the $D_T$ of DSS and dioxane remains relatively consistent over a range of pD values from 3.6 to 7.5. At 298 K and a pD of 3.6, the $D_T$ of DSS was $5.98\pm0.22 \times 10^{-10}$ m$^2$ s$^{-1}$, which was input into Equation 4 to give a $R_h$ of 3.47 Å. It is worth noting that DSS has been reported to be protonated at extremely low pH ("pH -6")[46] and can bind to some proteins[47] or possibly interact with other small molecules, such as urea,[12] indicating that

the diffusion properties of DSS will change under those conditions and therefore affect the utility of DSS as an internal viscosity standard. As expected and according to the Stokes-Einstein equation, the diffusion coefficient of DSS increases with temperature (Table 2 and Table 3); however, the accuracy of measured values for non-ambient temperatures (e.g. at 308 K) may be affected by thermal convection. This effect arises from the Rayleigh-Bernard instability and depends on the magnitude and the direction of the temperature gradient within the sample, as well as the geometry and physical properties of the sample.[48] Nonetheless, the $D_T$ of DSS remains relatively consistent from 288 K to 303 K. These results suggest that DSS is a suitable small molecule internal standard for diffusion measurements, particularly at ambient temperature, as performed in this study.

**Table 2:** Effect of pD and temperature on the diffusion measurements of small molecule internal standards 1,4-dioxane and DSS in 100% (v/v) $D_2O$.

| | **dioxane** | | **DSS** | | **dioxane/DSS** | |
|---|---|---|---|---|---|---|
| | $D_T$ ($10^{-10}$ $m^2$ $s^{-1}$)[a] | | $D_T$ ($10^{-10}$ $m^2$ $s^{-1}$)[a] | | $D_T$ ratio | |
| *Effect of pD*[b] | | | | | | |
| 3.7 | 9.68 | ±0.09 | 5.99 | ±0.07 | 1.62 | ±0.02 |
| 4.5 | 9.60 | ±0.08 | 5.93 | ±0.03 | 1.62 | ±0.02 |
| 5.5 | 9.60 | ±0.12 | 5.96 | ±0.04 | 1.61 | ±0.01 |
| 6.7 | 9.53 | ±0.09 | 5.93 | ±0.04 | 1.61 | ±0.02 |
| 7.4 | 9.65 | ±0.11 | 5.95 | ±0.06 | 1.62 | ±0.03 |
| *Effect of temperature (K)*[c] | | | | | | |
| 288 | 7.21 | ±0.05 | 4.44 | ±0.04 | 1.63 | ±0.01 |
| 293 | 8.33 | ±0.06 | 5.21 | ±0.01 | 1.60 | ±0.01 |
| 298 | 9.68 | ±0.11 | 5.99 | ±0.06 | 1.61 | ±0.03 |
| 303 | 10.97 | ±0.07 | 6.85 | ±0.04 | 1.60 | ±0.01 |
| 308 | 12.29 | ±0.08 | 7.96 | ±0.04 | 1.54 | ±0.01 |

[a] Diffusion coefficient reported as average and standard deviation of triplicate measurements

[b] Measurements conducted in 100% (v/v) $D_2O$ at 298 K

[c] Measurements conducted at pD 3.6

One advantage of PFG-NMR is the ability to use a large range of solvent systems. To measure $D_T$ for a range of cyclic peptides, we prepared samples in a mixture of $D_2O$ and acetonitrile, which is often used to improve the solubility of hydrophobic peptides. Before measuring the diffusion coefficients, we conducted molecular dynamics simulations of the peptides in water and in 30% (v/v) acetonitrile. Figure 3 shows a superposition of the cyclic peptide structures extracted from various time points of the simulation, showing that the presence or absence of acetonitrile only has a minor effect on the local structural flexibility of the cyclic peptides.

**Table 3:** Effect of pD and temperature on the diffusion measurements of small molecule internal standards 1,4-dioxane and DSS in 30% (v/v) acetonitrile-d3, 70% (v/v) $D_2O$.

| | **acetonitrile** | | **dioxane** | | **DSS** | | **dioxane/DSS** | |
|---|---|---|---|---|---|---|---|---|
| | $D_T$ ($10^{-10}$ $m^2$ $s^{-1}$)[a] | | $D_T$ ($10^{-10}$ $m^2$ $s^{-1}$)[a] | | $D_T$ ($10^{-10}$ $m^2$ $s^{-1}$)[a] | | $D_T$ ratio | |
| *Effect of pD*[b] | | | | | | | | |
| 3.6 | 15.35 | ±0.59 | 9.75 | ±0.35 | 5.98 | ±0.22 | 1.63 | ±0.03 |
| 4.5 | 15.43 | ±0.24 | 9.92 | ±0.24 | 6.00 | ±0.18 | 1.65 | ±0.03 |
| 5.5 | 15.82 | ±0.24 | 10.17 | ±0.21 | 6.22 | ±0.26 | 1.66 | ±0.01 |
| 6.4 | 14.99 | ±0.15 | 9.66 | ±0.11 | 5.86 | ±0.04 | 1.65 | ±0.03 |
| 7.5 | 15.56 | ±0.07 | 10.02 | ±0.14 | 5.90 | ±0.07 | 1.70 | ±0.01 |
| *Effect of temperature (K)*[c] | | | | | | | | |
| 288 | 11.76 | ±0.16 | 7.51 | ±0.07 | 4.47 | ±0.07 | 1.68 | ±0.01 |
| 293 | 13.41 | ±0.06 | 8.51 | ±0.16 | 5.04 | ±0.06 | 1.69 | ±0.04 |
| 298 | 15.35 | ±0.59 | 9.75 | ±0.35 | 5.98 | ±0.22 | 1.63 | ±0.03 |
| 303 | 17.22 | ±0.16 | 10.98 | ±0.23 | 6.73 | ±0.03 | 1.63 | ±0.04 |
| 308 | 20.80 | ±0.15 | 14.09 | ±0.07 | 9.17 | ±0.27 | 1.54 | ±0.04 |

[a] Diffusion coefficient reported as average and standard deviation of triplicate measurements

[b] Measurements conducted in 30% (v/v) acetonitrile-d3, 70% (v/v) $D_2O$ at 298 K

[c] Measurements conducted at pD 3.6

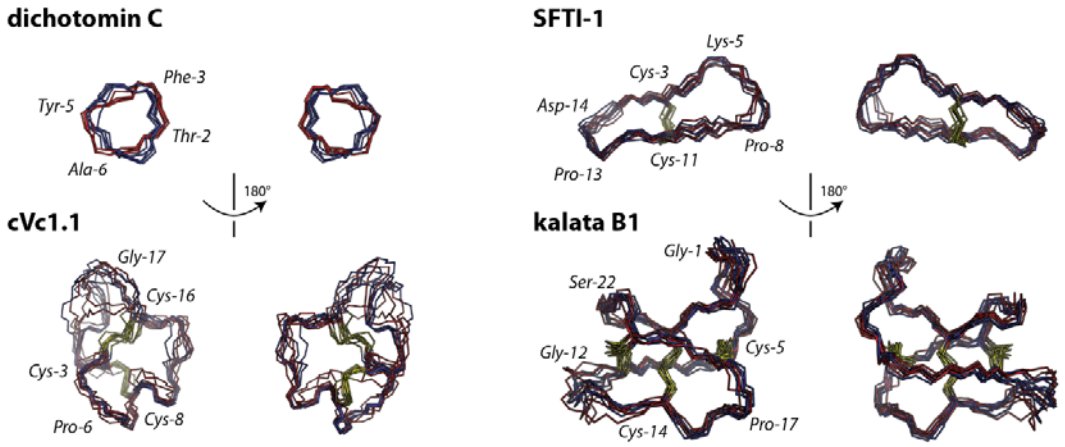


**Figure 3:** Molecular dynamics simulation of cyclic peptides. Backbone structures of cyclic peptides at selected time points of the simulation in water (colored blue) and in 30% (v/v) acetonitrile (colored red). Certain residues are labeled and the disulfide bonds, if present, are colored in yellow.

The $D_T$ values for a series of cyclic peptides were then measured in 100% (v/v) $D_2O$ and in 30% (v/v) acetonitrile-d3, 30% (v/v) $D_2O$ at two different pD values. As shown in Table 4, the $D_T$ values of the cyclic peptides and DSS were similar across the different solvent conditions tested. Importantly, the ratio of $D_T$ values of the peptide to DSS, a measure of the size of the peptide corrected for solvent viscosity, remains relatively consistent. One exception was observed for cVc1.1 in 30% (v/v) acetonitrile at pD 6.8, which might be due to a change in the size and shape of cVc1.1 or in the diffusion properties of DSS. The ratio of $D_T$ values of the peptide relative to dioxane was also calculated and is shown in Supplementary Table S1. Encouragingly, the measured $D_T$ values are consistent with predicted values using HYDROPRO, a computational algorithm that maps a hydrodynamic model to a known structure.[44] From the measured $D_T$ values we can then estimate the $R_h$ of the cyclic peptides using Equation 2 or Equation 3; the results are shown in Table 4. For Equation 2, which relies on interpretation of the absolute values of the measured $D_T$, errors in the calculated $R_h$ can arise from differences between the expected and actual sample temperature and solvent viscosity; the latter of the two variables might also be affected by solute concentration. Additionally, the measured $D_T$ is subject to errors both from inaccuracies in measuring the exact shape and strength of the gradient pulse and from spin-echo instability.[13] Therefore, Equation 3 has previously been

used to avoid these complexities.[12] It should be noted though that Equation 3 relies on accurate characterization of the diffusion properties of the internal standard and rests on the assumption that the $R_h$ of the standard is unchanged upon addition of the peptide. To validate the results obtained from Equation 3, different internal standards can be used to obtain a consensus result.[12] Nevertheless, $R_h$ values obtained from Equation 2 and 3 are similar and provide an estimate of the $R_h$ of the cyclic peptides in solution. As expected, there was a positive correlation between the number of residues of the cyclic peptide and its calculated hydrodynamic radius (Table 4 and Figure 4). For example, SFTI-1, a 14-residue cyclic peptide, had a $R_h$ of 8.77±0.05 Å, whereas kalata B1, a 29-residue cyclic peptide, had a $R_h$ of 10.64±0.16 Å.

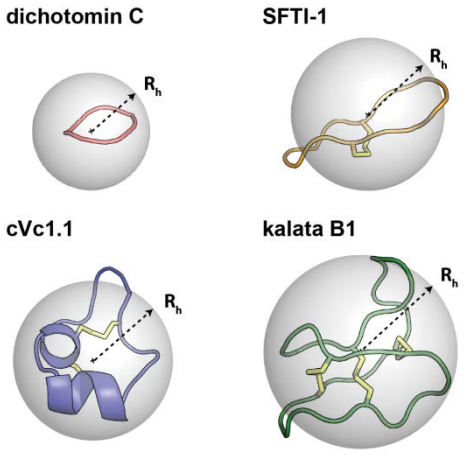


**Figure 4:** Schematic representation of the $R_h$ of cyclic peptides mapped onto their corresponding three-dimensional structures. The structures of the peptides are represented in ribbon representation and disulfides, if present, are colored in yellow. $R_h$ is shown as an arrow from the centre of mass, and as an overlapping sphere. The values for $R_h$ were calculated using Equation 3 and are shown in Table 4. Please note that the structures contain some degree of anisotropy and the sphere is only shown as a visual aid.

**Table 4:** Diffusion coefficients of cyclic peptides

| | $D_T$ ($10^{-10}$ $m^2$ $s^{-1}$)[b] | | | | $D_T$ ratio | | peptide $R_h$ (Å)[c] | | | |
|---|---|---|---|---|---|---|---|---|---|---|
| **solvent**[a] | Hydropro[d] | peptide | | DSS | | DSS/peptide | | Eq. 2 | | Eq. 3 | |
| **dichC** *(6 residues)* | | | | | | | | | | | |
| 100% $D_2O$, pD = 6.9 | 3.29 | 3.40 | ±0.04 | 5.97 | ±0.02 | 1.79 | ±0.02 | 5.85 | ±0.06 | 6.22 | ±0.07 |
| 30% $CD_3CN$, pD = 6.8 | | 3.60 | ±0.09 | 6.33 | ±0.16 | 1.76 | ±0.02 | 5.32 | ±0.14 | 5.86 | ±0.05 |
| 30% $CD_3CN$, pD = 3.7 | | 3.40 | ±0.04 | 6.02 | ±0.22 | 1.79 | ±0.03 | 5.72 | ±0.20 | 5.98 | ±0.10 |
| **SFTI-1** *(14 residues)* | | | | | | | | | | | |
| 100% $D_2O$, pD = 6.8 | 2.47 | 2.37 | ±0.01 | 5.99 | ±0.02 | 2.53 | ±0.05 | 8.36 | ±0.03 | 8.77 | ±0.05 |
| 30% $CD_3CN$, pD = 6.8 | | 2.45 | ±0.05 | 6.03 | ±0.02 | 2.46 | ±0.05 | 7.82 | ±0.15 | 8.23 | ±0.16 |
| 30% $CD_3CN$, pD = 3.6 | | 2.35 | ±0.11 | 5.79 | ±0.09 | 2.46 | ±0.11 | 8.15 | ±0.37 | 8.22 | ±0.34 |
| **cVc1.1** *(22 residues)* | | | | | | | | | | | |
| 100% $D_2O$, pD = 6.8 | 2.25 | 2.18 | ±0.03 | 5.84 | ±0.01 | 2.70 | ±0.04 | 9.17 | ±0.16 | 9.36 | ±0.15 |
| 30% $CD_3CN$, pD = 6.8 | | 2.18 | ±0.07 | 5.55 | ±0.08 | 2.55 | ±0.08 | 8.78 | ±0.28 | 8.50 | ±0.26 |
| 30% $CD_3CN$, pD = 3.4 | | 2.22 | ±0.01 | 5.97 | ±0.10 | 2.71 | ±0.03 | 8.69 | ±0.08 | 9.03 | ±0.12 |
| **kB1** *(29 residues)* | | | | | | | | | | | |
| 100% $D_2O$, pD = 6.8 | 2.07 | 1.95 | ±0.03 | 5.98 | ±0.02 | 3.07 | ±0.05 | 10.18 | ±0.14 | 10.64 | ±0.16 |
| 30% $CD_3CN$, pD = 6.8 | | 1.99 | ±0.03 | 5.98 | ±0.03 | 3.01 | ±0.04 | 9.63 | ±0.13 | 10.04 | ±0.09 |
| 30% $CD_3CN$, pD = 3.6 | | 2.06 | ±0.04 | 6.03 | ±0.02 | 2.93 | ±0.04 | 9.30 | ±0.14 | 9.76 | ±0.15 |

[a] Three solvent systems were used: 100% v/v $D_2O$ (100% $D_2O$) at pD ~7; 30% v/v acetonitrile-d3, 70% v/v $D_2O$ (30% $CD_3CN$) at pD ~7; and 30% v/v acetonitrile-d3, 70% v/v $D_2O$ (30% $CD_3CN$) at pD ~3. The concentrations of SFTI-1 and cVc1.1 were 1.40 and 1.20 mM, respectively. The concentration of dichC was 0.47 mM in 100% (v/v) $D_2O$ and 1.01 mM in the other two solvents. The concentration of kB1 was 0.3 mM in 100% (v/v) $D_2O$ and 0.98 mM in the other two solvents. The concentration of dichC and kB1 were lower in the absence of acetonitrile in the solvent because of reduced solubility.

[b] Diffusion coefficient reported as average and standard deviation of triplicate measurements at 298 K

[c] Evaluated using Equation 2 and 3 (Experimental Methods)

[d] Computed using the program HYDROPRO[44] (Experimental Methods)

We were further interested in using diffusion measurements to study self-association of cyclic peptides. We focused on kalata B2, a cyclic plant peptide that possesses potent insecticidal activity.[33] Previous analytical ultracentrifugation studies suggest that self-association of kalata B2 might play an important role in its mechanism of action.[49] Diffusion measurements of kalata B2 were conducted in $D_2O$ at different peptide concentrations. As shown in Table 5, the calculated $R_h$ of kalata B2 increased with increasing peptide concentration. More specifically, at 0.22 mM, kalata B2 was mostly or completely monomeric, with a $D_T$ of

2.01±0.02 × $10^{-10}$ $m^2$ $s^{-1}$ and a calculated $R_h$ of 10.43±0.13 Å (which is similar to the value measured for kalata B1), but at 1.70 mM, there was strong evidence of self-association, which was indicated by a significantly smaller $D_T$ of 1.22±0.03 × $10^{-10}$ $m^2$ $s^{-1}$ and a larger $R_h$ of 17.06±0.22 Å. Interestingly, this result suggests that kalata B2 forms a tetramer and is consistent with a predicted $D_T$ of 1.15× $10^{-10}$ $m^2$ $s^{-1}$ using HYDROPRO[44] and a computational model of the tetramer.[50] Furthermore, in the presence of 30% (v/v) acetonitrile-d3 and at 1.5 mM peptide concentration, a concentration expected to induce self-association, kalata B2 was largely monomeric, as indicated by a calculated $R_h$ of 10.25±0.11 Å (Table 5). This finding is probably due to ability of acetonitrile to disrupt the hydrophobic interactions between individual kalata B2 molecules that have recently been suggested to be responsible for kalata B2 self-association in solution.[50] Overall, these studies show that diffusion measurements are sensitive to the supra-molecular structure of cyclic peptides and, therefore, is a valuable tool for characterizing oligomerization of cyclic peptides.

**Table 5:** Diffusion measurements of the self-association of kalata B2

| **peptide concentration** | **DSS** | | **kalata B2** *(29 residues)* | | | | | |
|---|---|---|---|---|---|---|---|---|
| **(mM)** | $D_T$ ($10^{-10}$ $m^2$ $s^{-1}$)[d] | | $D_T$ ($10^{-10}$ $m^2$ $s^{-1}$)[c] | | Eq. 2: $R_h$ (Å)[e] | | Eq. 3: $R_h$ (Å)[f] | |
| 1.50[a] | 5.91 | ±0.42 | 2.08 | ±0.16 | 9.58 | ±0.71 | 9.86 | ±0.05 |
| 1.50[b] | 5.91 | ±0.21 | 2.00 | ±0.08 | 9.93 | ±0.38 | 10.25 | ±0.11 |
| 0.22[c] | 6.06 | ±0.12 | 2.01 | ±0.02 | 9.85 | ±0.76 | 10.43 | ±0.13 |
| 0.28[c] | 6.02 | ±0.01 | 1.86 | ±0.01 | 10.70 | ±0.09 | 11.26 | ±0.10 |
| 0.61[c] | 6.03 | ±0.02 | 1.53 | ±0.02 | 12.95 | ±0.14 | 13.66 | ±0.12 |
| 1.10[c] | 5.93 | ±0.20 | 1.34 | ±0.02 | 14.78 | ±0.16 | 15.33 | ±0.36 |
| 1.70[c] | 5.98 | ±0.15 | 1.22 | ±0.03 | 16.30 | ±0.33 | 17.06 | ±0.22 |

[a] Diffusion measurements in 30% (v/v) acetonitrile-d3, 70% (v/v) $D_2O$, pD 3.6, 298K

[b] Diffusion measurements in 30% (v/v) acetonitrile-d3, 70% (v/v) $D_2O$, pD 6.9, 298K

[c] Diffusion measurements in 100% (v/v) $D_2O$, pD 6.9, 298K

[d] Diffusion coefficient reported as average and standard deviation of triplicate measurements

[e] Evaluated using Equation 2 (Experimental Methods)

[f] Evaluated using Equation 3 (Experimental Methods) and DSS as an internal standard

## Conclusions

In conclusion, we have conducted fundamental studies on the diffusion properties of a range of small cyclic peptides that have therapeutic potential. We demonstrated that using internal standards, such as DSS, the hydrodynamic radius of cyclic peptides can be characterized, providing information on solvent and shape effects on motion in different solvent solutions. In a recent study on proteins, the hydrodynamic radius was compared to other radii terms, such as the radius of gyration, to investigate protein shape and flexibility.[51] We postulate that a similar method could be used to characterize structures of cyclic peptides (an analysis of radii terms is shown in Supplementary Tables S2 and S3). We further postulate that diffusion measurements are likely to be useful in exploring the effect of shape on the diffusion of cyclic peptide drug leads through a membrane, which would facilitate the development of new rules to guide the design of drugs using this emerging molecule class. Furthermore, we demonstrated that diffusion measurements can be applied to understand the self-association behavior of cyclic peptides, which may provide structural insight into their mechanism of action. The ability to characterize interactions of cyclic peptides with each other suggests that diffusion measurements are likely to be useful for studying the interaction of cyclic peptides with a molecular target, which may assist in guiding future drug design efforts using cyclic peptides as templates.

**Acknowledgements**

We thank Olivier Cheneval and Phillip Walsh for help with peptide synthesis. This work was supported by an ARC Linkage Grant (LP110200213) co-funded by Pfizer and a Queensland Government Smart Futures Co-investment Grant. CKW was supported by a National Health and Medical Research Council (NHMRC) Early Career Research Fellowship (546578). JES is a NHMRC Early Career Fellow (APP1069819). DJC is a NHMRC Professorial Fellow (APP1026501).

**Supporting Information Available**

Additional experimental details about analysis of translational diffusion induced signal attenuation (Equations S1 and S2) and prediction of radii terms (Equations S3-S7); translational diffusion of dioxane (Figure S1); one and two-component fits of translational diffusion induced signal attenuation (Figure S2); diffusion properties of cyclic peptides and internal standards (Table S1); structural properties of cyclic peptides (Table S2); ratio of equivalent radii of cyclic peptides compared to proteins (Table S3). This information is available free of charge via the Internet at http://pubs.acs.org.

**References**


(1) Price, W. S. Pulsed-Field Gradient Nuclear Magnetic Resonance as a Tool for Studying Translational Diffusion: Part 1. Basic Theory. *Concepts Magn. Reson.* **1997**, *9*, 299-336.

(2) Horst, R.; Horwich, A. L.; Wuthrich, K. Translational Diffusion of Macromolecular Assemblies Measured Using Transverse-Relaxation-Optimized Pulsed Field Gradient Nmr. *J. Am. Chem. Soc.* **2011**, *133*, 16354-16357.

(3) Krishnan, V. J. Determination of Oligomeric State of Proteins in Solution from Pulsed-Field-Gradient Self-Diffusion Coefficient Measurements. A Comparison of Experimental, Theoretical, and Hard-Sphere Approxmiated Values. *J. Magn. Reson.* **1997**, *124*, 468-473.

(4) Ilyina, E.; Roongta, V.; Pan, H.; Woodward, C.; Mayo, K. H. A Pulsed-Field Gradient Nmr Study of Bovine Pancreatic Trypsin Inhibitor Self-Association. *Biochemistry* **1997**, *36*, 3383-3388.

(5) Dingley, A. J.; Mackay, J. P.; Chapman, B. E.; Morris, M. B.; Kuchel, P. W.; Hambly, B. D.; King, G. F. Measuring Protein Self-Association Using Pulsed-Field-Gradient Nmr Spectroscopy: Application to Myosin Light Chain 2. *J. Biomol. NMR* **1995**, *6*, 321-328.

(6) Yao, S.; Howlett, G. J.; Norton, R. S. Peptide Self-Association in Aqueous Trifluoroethanol Monitored by Pulsed Field Gradient Nmr Diffusion Measurements. *J. Biomol. NMR* **2000**, *16*, 109-119.

(7) Li, C.; Wang, Y.; Pielak, G. J. Translational and Rotational Diffusion of a Small Globular Protein under Crowded Conditions. *J. Phys. Chem. B* **2009**, *113*, 13390-13392.

(8) Hajduk, P. J.; Olejniczak, E. T.; Fesik, S. W. One-Dimensional Relaxation- and Diffuision-Edited Nmr Methods for Screening Compounds That Bind to Macromolecules. *J. Am. Chem. Soc.* **1998**, *119*, 12257-12261.

(9) Tillett, M. L.; Horsfield, M. A.; Lian, L. Y.; Norwood, T. J. Protein-Ligand Interactions Measured by 15n-Filtered Diffusion Experiments. *J. Biomol. NMR* **1999**, *13*, 223-232.

(10) Vinogradova, O.; Sonnichsen, F.; Sanders, C. R., 2nd. On Choosing a Detergent for Solution Nmr Studies of Membrane Proteins. *J. Biomol. NMR* **1998**, *11*, 381-386.

(11) Chou, J. J.; Baber, J. L.; Bax, A. Characterization of Phospholipid Mixed Micelles by Translational Diffusion. *J. Biomol. NMR* **2004**, *29*, 299-308.

(12) Jones, J. A.; Wilkins, D. K.; Smith, L. J.; Dobson, C. M. Characterisation of Protein Unfolding by Nmr Diffusion Measurements. *J. Biomol. NMR* **1997**, *10*, 199-203.

(13) Wilkins, D. K.; Grimshaw, S. B.; Receveur, V.; Dobson, C. M.; Jones, J. A.; Smith, L. J. Hydrodynamic Radii of Native and Denatured Proteins Measured by Pulse Field Gradient Nmr Techniques. *Biochemistry* **1999**, *38*, 16424-16431.

(14) Arnison, P. G.; Bibb, M. J.; Bierbaum, G.; Bowers, A. A.; Bugni, T. S.; Bulaj, G.; Camarero, J. A.; Campopiano, D. J.; Challis, G. L.; Clardy, J.*et al.* Ribosomally Synthesized and Post-Translationally Modified Peptide Natural Products: Overview and Recommendations for a Universal Nomenclature. *Nat. Prod. Rep.* **2013**, *30*, 108-160.

(15) Wang, C. K.; Kaas, Q.; Chiche, L.; Craik, D. J. Cybase: A Database of Cyclic Protein Sequences and Structures, with Applications in Protein Discovery and Engineering. *Nucleic Acids Res.* **2008**, *36*, D206-210.

(16) Goransson, U.; Burman, R.; Gunasekera, S.; Stromstedt, A. A.; Rosengren, K. J. Circular Proteins from Plants and Fungi. *J. Biol. Chem.* **2012**, *287*, 27001-27006.

(17) Craik, D. J.; Fairlie, D. P.; Liras, S.; Price, D. The Future of Peptide-Based Drugs. *Chem. Biol. Drug Des.* **2013**, *81*, 136-147.

(18) Clark, R. J.; Jensen, J.; Nevin, S. T.; Callaghan, B. P.; Adams, D. J.; Craik, D. J. The Engineering of an Orally Active Conotoxin for the Treatment of Neuropathic Pain. *Angew. Chem. Int. Ed. Engl.* **2010**, *49*, 6545-6548.

(19) Lesner, A.; Legowska, A.; Wysocka, M.; Rolka, K. Sunflower Trypsin Inhibitor 1 as a Molecular Scaffold for Drug Discovery. *Curr. Pharm. Des.* **2011**, *17*, 4308-4317.

(20) Craik, D. J.; Daly, N. L.; Bond, T.; Waine, C. Plant Cyclotides: A Unique Family of Cyclic and Knotted Proteins That Defines the Cyclic Cystine Knot Structural Motif. *J. Mol. Biol.* **1999**, *294*, 1327-1336.

(21) Craik, D. J.; Swedberg, J. E.; Mylne, J. S.; Cemazar, M. Cyclotides as a Basis for Drug Design. *Expert Opin. Drug Discov.* **2012**, *7*, 179-194.

(22) Wang, C. K.; Gruber, C. W.; Cemazar, M.; Siatskas, C.; Tagore, P.; Payne, N.; Sun, G.; Wang, S.; Bernard, C. C.; Craik, D. J. Molecular Grafting onto a Stable Framework Yields Novel Cyclic Peptides for the Treatment of Multiple Sclerosis. *ACS Chem. Biol.* **2013**.

(23) Wong, C. T.; Rowlands, D. K.; Wong, C. H.; Lo, T. W.; Nguyen, G. K.; Li, H. Y.; Tam, J. P. Orally Active Peptidic Bradykinin B1 Receptor Antagonists Engineered from a Cyclotide Scaffold for Inflammatory Pain Treatment. *Angew. Chem. Int. Ed. Engl.* **2012**, *51*, 5620-5624.

(24) Pei, H.; Germann, M. W.; Allison, S. A. Translational Diffusion Constants of Short Peptides: Measurement by Nmr and Their Use in Structural Studies of Peptides. *J. Phys. Chem. B* **2009**, *113*, 9326-9329.

(25) Shenkarev, Z. O.; Nadezhdin, K. D.; Sobol, V. A.; Sobol, A. G.; Skjeldal, L.; Arseniev, A. S. Conformation and Mode of Membrane Interaction in Cyclotides. Spatial Structure of Kalata B1 Bound to a Dodecylphosphocholine Micelle. *FEBS J.* **2006**, *273*, 2658-2672.

(26) Wang, C. K.; Colgrave, M. L.; Ireland, D. C.; Kaas, Q.; Craik, D. J. Despite a Conserved Cystine Knot Motif, Different Cyclotides Have Different Membrane Binding Modes. *Biophys. J.* **2009**, *97*, 1471-1481.

(27) Conibear, A. C.; Rosengren, K. J.; Harvey, P. J.; Craik, D. J. Structural Characterization of the Cyclic Cystine Ladder Motif of Theta-Defensins. *Biochemistry* **2012**, *51*, 9718-9726.

(28) Morita, H.; Kayashita, T.; Shishido, A.; Takeya, K.; Itokawa, H.; Shiro, M. Dichotomins a - E, New Cyclic Peptides from *Stellaria Dichotoma* L. Var. *Lanceolata* Bge. *Tetrahedron* **1996**, *52*, 1165-1176.

(29) Luckett, S.; Garcia, R. S.; Barker, J. J.; Konarev, A. V.; Shewry, P. R.; Clarke, A. R.; Brady, R. L. High-Resolution Structure of a Potent, Cyclic Proteinase Inhibitor from Sunflower Seeds. *J. Mol. Biol.* **1999**, *290*, 525-533.

(30) Gran, L. Oxytocic Principles of Oldenlandia Affinis. *Lloydia* **1973**, *36*, 174-178.

(31) Colgrave, M. L.; Kotze, A. C.; Huang, Y. H.; O'Grady, J.; Simonsen, S. M.; Craik, D. J. Cyclotides: Natural, Circular Plant Peptides That Possess Significant Activity against Gastrointestinal Nematode Parasites of Sheep. *Biochemistry* **2008**, *47*, 5581-5589.

(32) Plan, M. R.; Saska, I.; Cagauan, A. G.; Craik, D. J. Backbone Cyclised Peptides from Plants Show Molluscicidal Activity against the Rice Pest Pomacea Canaliculata (Golden Apple Snail). *J. Agric. Food Chem.* **2008**, *56*, 5237-5241.

(33) Jennings, C. V.; Rosengren, K. J.; Daly, N. L.; Plan, M.; Stevens, J.; Scanlon, M. J.; Waine, C.; Norman, D. G.; Anderson, M. A.; Craik, D. J. Isolation, Solution Structure, and Insecticidal Activity of Kalata B2, a Circular Protein with a Twist: Do Mobius Strips Exist in Nature? *Biochemistry* **2005**, *44*, 851-860.

(34) Gustafson, K. R.; McKee, T. C.; Bokesch, H. R. Anti-Hiv Cyclotides. *Curr. Protein Pept. Sci.* **2004**, *5*, 331-340.

(35) Grundemann, C.; Thell, K.; Lengen, K.; Garcia-Kaufer, M.; Huang, Y. H.; Huber, R.; Craik, D. J.; Schabbauer, G.; Gruber, C. W. Cyclotides Suppress Human T-Lymphocyte Proliferation by an Interleukin 2-Dependent Mechanism. *PLoS One* **2013**, *8*, e68016.

(36) Krezel, A.; Bal, W. A Formula for Correlating Pka Values Determined in D2o and H2o. *J. Inorg. Biochem.* **2004**, *98*, 161-166.

(37) Wu, D.; Chen, A.; Johnson, C. S. An Improved Diffusion-Ordered Spectroscopy Experiment Incorporating Bipolar-Gradient Pulses. *J. Magn. Reson.* **1995**, *115*.

(38) Stejskal, E. O.; Tanner, J. E. Spin Diffusion Measurements: Spin Echos in the Presence of a Time-Dependent Field Gradient. *J. Chem. Phys.* **1965**, *42*, 288-292.

(39) Kuchel, P. W.; Pagès, G.; Nagashima, K.; Velan, S.; Vijayaragavan, V.; Nagarajan, V.; Chuang, K. H. Stejskal-Tanner Equation Derived in Full. *Concepts Magn. Reson.* **2012**, *40A*, 205-214.

(40) Sinnaeve, D. The Stejskal-Tanner Equation Generalized for Any Gradient Shape - an Overview of Most Pulse Sequences Measuring Free Diffusion. *Concepts Magn. Reson.* **2012**, *40A*, 39-65.

(41) Harris, K. R.; Woolf, L. A. Temperature and Volume Dependence of the Viscosity of Water and Heavy Water at Low Temperatures. *J. Chem. Eng. Data* **2004**, *49*, 1064-1069.

(42) Thompson, J. W.; Kaiser, T. J.; Jorgenson, J. W. Viscosity Measurements of Methanol-Water and Acetonitrile-Water Mixtures at Pressures up to 3500 Bar Using Anovel Capillary Time-of-Flight Viscometer. *J. Chromatogr. A* **2006**, *1134*, 201-209.

(43) Kaas, Q.; Westermann, J. C.; Halai, R.; Wang, C. K.; Craik, D. J. Conoserver, a Database for Conopeptide Sequences and Structures. *Bioinformatics* **2008**, *24*, 445-446.

(44) Garcia De La Torre, J.; Huertas, M. L.; Carrasco, B. Calculation of Hydrodynamic Properties of Globular Proteins from Their Atomic-Level Structure. *Biophys. J.* **2000**, *78*, 719-730.

(45) Northfield, S. E.; Wang, C. K.; Schroeder, C. I.; Durek, T.; Kan, M. W.; Swedberg, J. E.; Craik, D. J. Disulfide-Rich Macrocyclic Peptides as Templates in Drug Design. *Eur. J. Med. Chem.* **2014**, *77*, 248-257.

(46) Koeberg-Telder, A.; Cerfontain, H. *J. Chem. Soc. Perkin Trans. 2* **1975**, 226-229.

(47) Laurents, D. V.; Gorman, P. M.; Guo, M.; Rico, M.; Chakrabartty, A.; Bruix, M. Alzheimer's Abeta40 Studied by Nmr at Low Ph Reveals That Sodium 4,4-Dimethyl-4-Silapentane-1-Sulfonate (Dss) Binds and Promotes Beta-Ball Oligomerization. *J. Biol. Chem.* **2005**, *280*, 3675-3685.

(48) Goux, W. J.; Verkruyse, L. A.; Salter, S. J. The Impact of Rayleigh-Bénard Convection on Nmr Pulsed-Field-Gradient Diffusion Measurements. *J. Magn. Reson.* **1990**, *88*, 609-614.

(49) Nourse, A.; Trabi, M.; Daly, N. L.; Craik, D. J. A Comparison of the Self-Association Behavior of the Plant Cyclotides Kalata B1 and Kalata B2 Via Analytical Ultracentrifugation. *J. Biol. Chem.* **2004**, *279*, 562-570.

(50) Rosengren, K. J.; Daly, N. L.; Harvey, P. J.; Craik, D. J. The Self-Association of the Cyclotide Kalata B2 in Solution Is Guided by Hydrophobic Interactions. *Biopolymers* **2013**, *100*, 453-460.

(51) Ortega, A.; Garcia de la Torre, J. Equivalent Radii and Ratios of Radii from Solution Properties as Indicators of Macromolecular Conformation, Shape, and Flexibility. *Biomacromolecules* **2007**, *8*, 2464-2475.

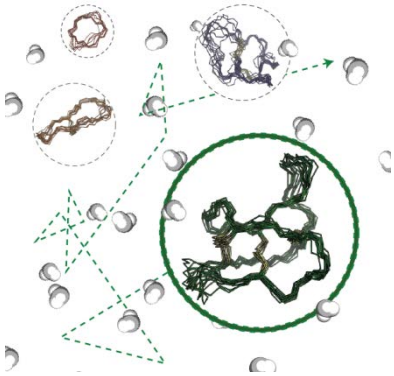

**Table of Contents Figure**